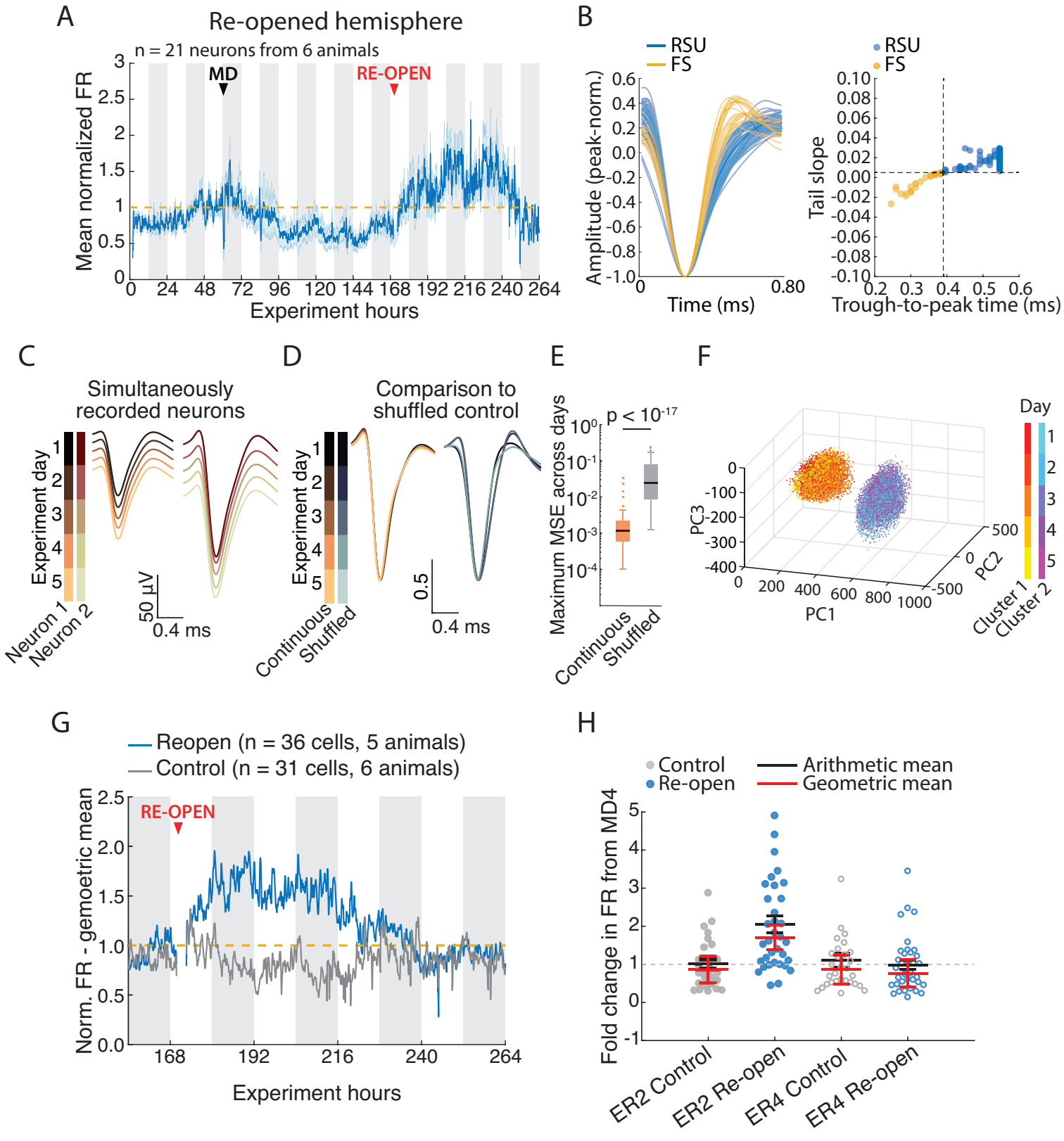
A
Re-opened hemisphere
n = 21 neurons from 6 animals
MD
RE-OPEN
Mean normalized FR
Experiment hours
B
RSU
FS
Amplitude (peak-norm.)
Time (ms)
Tail slope
Trough-to-peak time (ms)
C
Simultaneously recorded neurons
Experiment day
Neuron 1
Neuron 2
50 µV
0.4 ms
D
Comparison to shuffled control
Continuous
Shuffled
0.5
0.4 ms
E
p < 10-17
Maximum MSE across days
Continuous
Shuffled
F
Day
PC1
PC2
PC3
Cluster 1
Cluster 2
G
Reopen (n = 36 cells, 5 animals)
Control (n = 31 cells, 6 animals)
RE-OPEN
Norm. FR - gemoetric mean
Experiment hours
H
Control
Re-open
Arithmetic mean
Geometric mean
Fold change in FR from MD4
ER2 Control
ER2 Re-open
ER4 Control
ER4 Re-open

Figure S1: Continuous recordings of V1 neuronal activity in freely behaving rats, Related to Figure 1. **A.** Average FR, normalized to baseline (hours 36-60), for all neurons recorded continuously in the deprived/re-opened hemisphere for 11 days throughout baseline, MD and ER. Yellow dashed line indicates mean baseline FR. Labeled arrows indicate time of MD and ER. White/gray boxes in background denote 12-hour periods of light/dark. **B.** Left, average waveforms for recorded regular-spiking units (RSU, blue) and putative fast-spiking cells (FS, yellow). Right, illustration of the criteria used to separate RSU and FS units. Dashed lines indicate thresholds for Tail slope and Trough-to-peak time. **C.** Daily average waveforms (WFs) for two RSUs (putative excitatory neurons) recorded simultaneously on the same wire for 5 days (MD4 to ER4). Note similarity of WFs across days, and discriminability between the two neurons. **D.** Example peak-scaled daily average WFs for a continuously recorded neuron (left) and a shuffled random unit (right). See STAR methods for details ("Automated spike extraction, clustering and sorting"). **E.** Result of bootstrap analysis (see STAR methods for details). Maximum mean-squared-error (MSE) between daily peak-scaled average WFs for continuous vs shuffled random units. Two-sample t-test, $p < 10^{-17}$. **F.** Visualization of clustering output for two example units recorded on the same wire. Each dot represents a waveform (for visualization purposes, only a subset of dots are shown), and dots are color-coded by recording day. **G.** Main effect of eye re-opening on FR of RSUs in both hemispheres, calculated using geometric means, instead of arithmetic means. The main effect is visible (compare to Fig 1D), indicating it is not an artifact of using arithmetic methods for calculations. **H.** Fold change in FR on ER2 and ER4 for neurons in both hemispheres. Black lines show arithmetic means, red lines show geometric means.

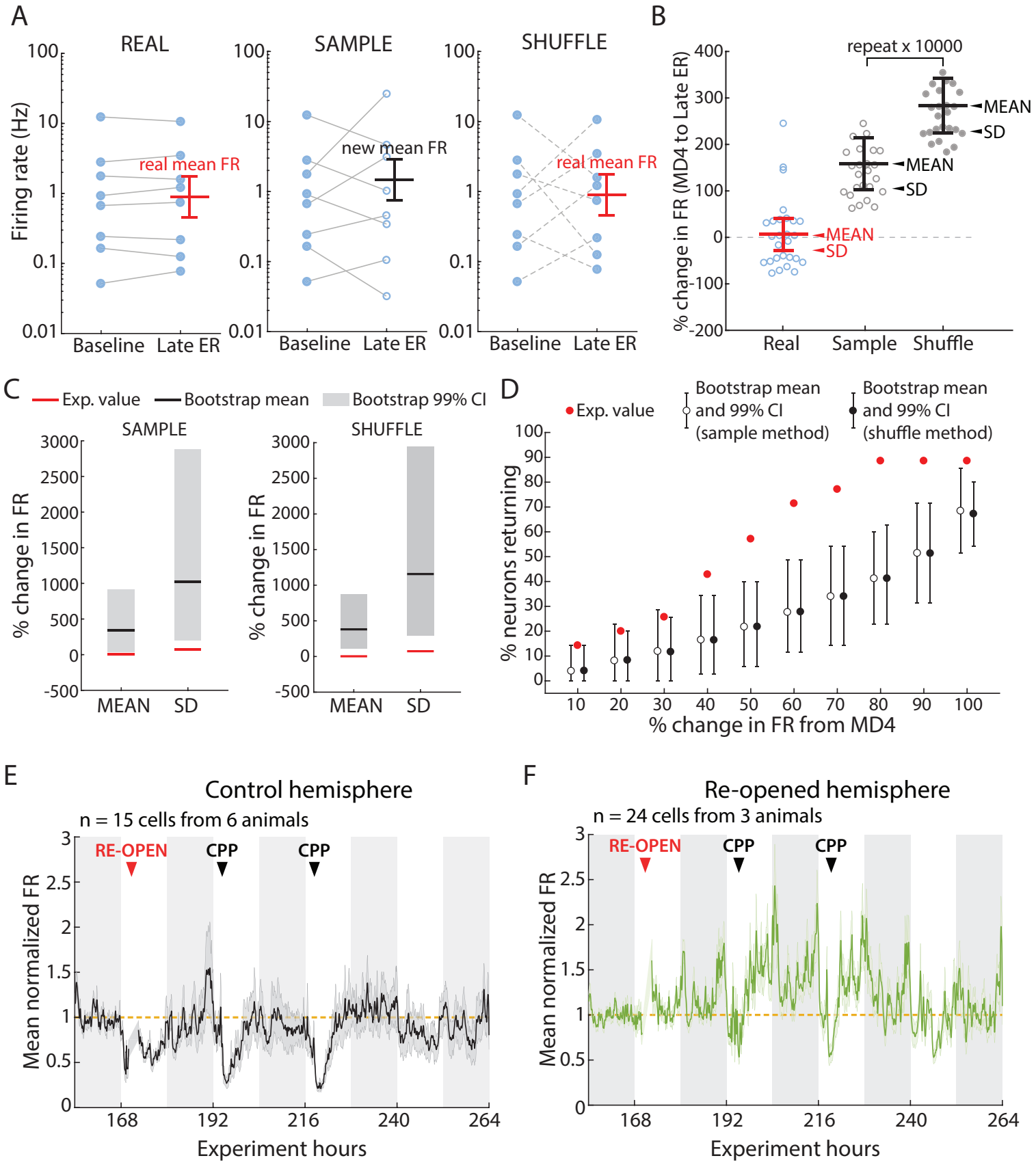
A
REAL
SAMPLE
SHUFFLE
Firing rate (Hz)
real mean FR
new mean FR
Baseline
Late ER
B
repeat x 10000
% change in FR (MD4 to Late ER)
MEAN
SD
Real
Sample
Shuffle
C
Exp. value
Bootstrap mean
Bootstrap 99% CI
% change in FR
MEAN
SD
D
Exp. value
Bootstrap mean and 99% CI (sample method)
Bootstrap mean and 99% CI (shuffle method)
% neurons returning
% change in FR from MD4
E
Control hemisphere
n = 15 cells from 6 animals
RE-OPEN
CPP
Mean normalized FR
Experiment hours
F
Re-opened hemisphere
n = 24 cells from 3 animals

Figure S2: Neurons recover to their initial baseline FR after ER-induced overshoot, Related to Figures 1 and 2. **A.** Diagram illustrating the two bootstrap methods used (see STAR methods, "Bootstrap analysis of FR recovery", for details). Reference data (left) are the baseline and late ER distribution of FRs in the re-opened hemisphere (shown is an illustration of the data, see Figure 1G for real data). Red line and error bars denote real mean FR of the distribution at late ER. We simulated a new ER4 distribution and paired neurons from the real MD4 distribution to these new simulated FR values. Bootstrap analysis with the "Sample" method (middle panel) simulates an ER4 distribution by sampling from the interpolated real ER4 distribution, thus resulting in distributions with a mean FR different than real data. Bootstrap analysis with the "Shuffle" method (right panel), shuffles the real ER4 distribution, thus resulting in a new distribution with mean FR equal to the real data. **B.** Quantification of bootstrap analysis. For each sampling or shuffling iteration the % change in FR from baseline is computed for each neuron, and the resulting mean and standard deviation (SD) of the distribution are calculated. This is repeated over 10,000 iterations to obtain confidence intervals (CI) for the mean and SD. **C.** Bootstrap analysis results for sample (left) and shuffle (right) methods. The red line indicates real mean and SD for the data in Figure 1F. Black lines indicate average values over 10,000 bootstrap iterations. Gray shaded area indicates the 99% CI for mean and SD. **D.** Estimate of the FR range over which neurons vary their FR, compared to bootstrap control (see STAR methods, "Bootstrap analysis of FR recovery", for details). Red dots indicate experimental value, and means and 99% CIs for sample (open circles) and shuffle (filled circles) methods are shown. **E.** Acute effect of CPP injections on FRs in V1 (control hemisphere)*.* Average baseline-normalized FR for neurons recorded in the control hemisphere of animals injected with CPP during recovery of FR after ER. CPP injections (labeled black arrows) briefly depress FRs, but cause no long-lasting effects in the control hemisphere. Dashed yellow line indicates baseline FR. **F.** Acute effect of CPP injections on FRs in V1 (re-opened

hemisphere). CPP injections (labeled black arrows) have the same acute effect, but FRs still show overshoot and recovery following ER.

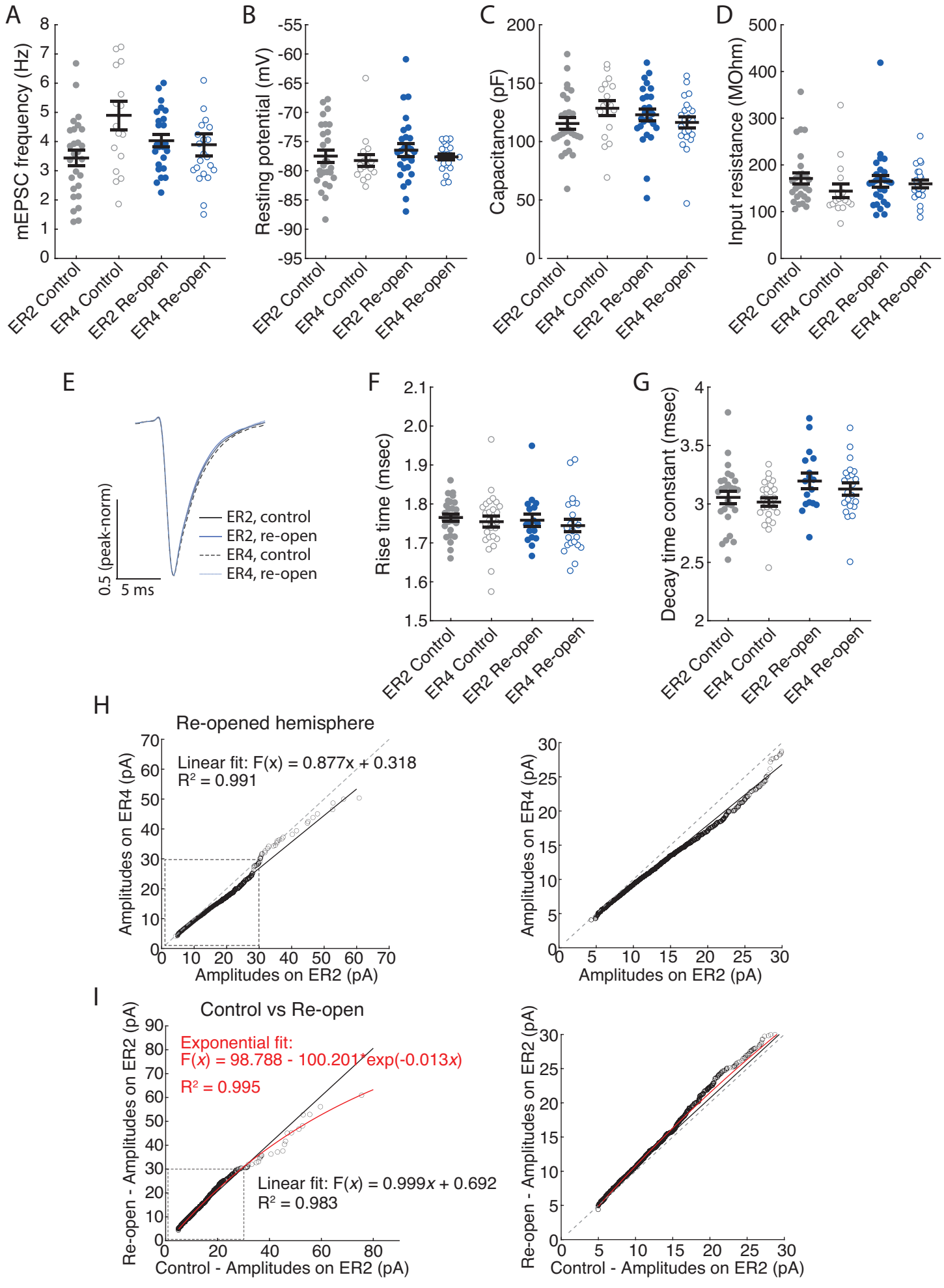
A
mEPSC frequency (Hz)
B
Resting potential (mV)
C
Capacitance (pF)
D
Input resistance (MOhm)
ER2 Control
ER4 Control
ER2 Re-open
ER4 Re-open
E
0.5 (peak-norm)
5 ms
ER2, control
ER2, re-open
ER4, control
ER4, re-open
F
Rise time (msec)
G
Decay time constant (msec)
H
Re-opened hemisphere
Linear fit: F(x) = 0.877x + 0.318
R² = 0.991
Amplitudes on ER4 (pA)
Amplitudes on ER2 (pA)
I
Control vs Re-open
Exponential fit:
F(x) = 98.788 - 100.201*exp(-0.013x)
R² = 0.995
Linear fit: F(x) = 0.999x + 0.692
R² = 0.983
Re-open - Amplitudes on ER2 (pA)
Control - Amplitudes on ER2 (pA)

Figure S3. ER does not cause change in passive properties or mEPSC kinetics, Related to Figure 3. **A – D.** Passive neuronal properties for all cells recorded in each condition. No change in mEPSC frequency (A), resting membrane potential (B), cell capacitance (C) or input resistance (D). Kruskal-Wallis test with Tukey-Kramer post-hoc, no significant results. **E.** Peak-scaled average mEPSC waveforms for each condition, overlaid. **F, G.** Summary of waveform kinetics for all cells in each condition. No change in rise time (F) or decay time constant (G). **H.** Sorted mEPSC amplitudes at ER2 vs ER4 in the re-opened hemisphere, showing scaling relationship. Dashed line is the unity line, solid line indicates linear fit and each open circle is one mEPSC event. Panel on the right shows zoomed-in view of are within dashed rectangle (0 – 30 pA). **I.** Sorted mEPSC amplitudes in the control vs re-opened hemispheres at ER2. In this case the data are better fit by an exponential than a linear function. Scaling the control distribution by a linear function does not recover the re-opened distribution (see Figure 3F). Black solid line indicates linear fit, red solid line indicates exponential fit and open circles are individual mEPSC events.

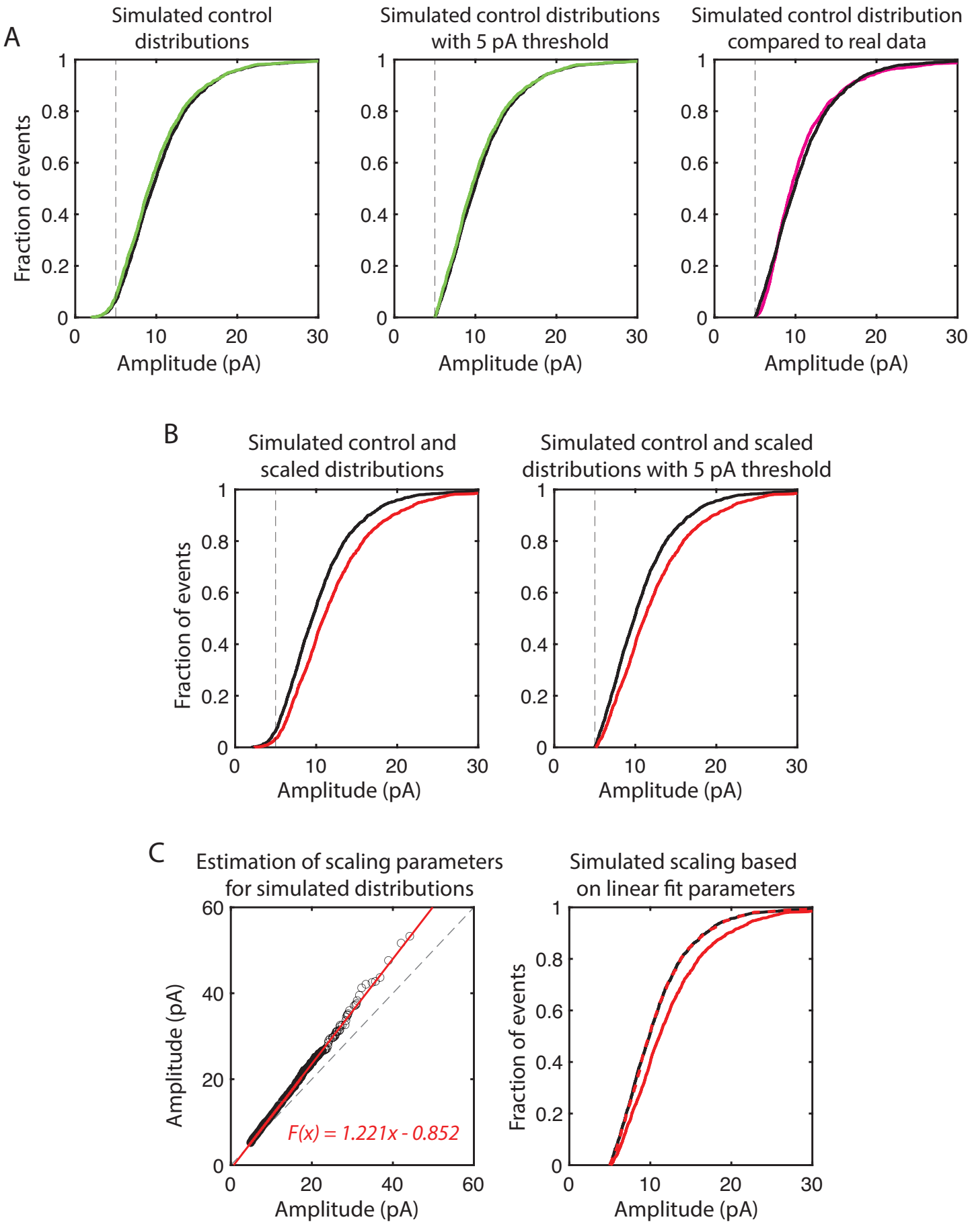
A
Simulated control distributions
Simulated control distributions with 5 pA threshold
Simulated control distribution compared to real data
Fraction of events
Amplitude (pA)
B
Simulated control and scaled distributions
Simulated control and scaled distributions with 5 pA threshold
Fraction of events
Amplitude (pA)
C
Estimation of scaling parameters for simulated distributions
Simulated scaling based on linear fit parameters
F(x) = 1.221x - 0.852
Amplitude (pA)
Fraction of events
Amplitude (pA)

Figure S4: Simulation of mEPSC analysis for perfect multiplicative scaling, Related to Figure 3. **A.** To simulate perfect multiplicative scaling, we created two control distributions based on realistic structural data for number of synapses and AMPARs (see STAR methods for details). We randomly sampled the two control distributions until they were different from each other ($p < 0.05$, Kolmogorov-Smirnov test, left panel). Dashed line indicates 5 pA threshold, corresponding to the event detection threshold in our experimental setup. Center panel shows the simulated control distributions truncated at the 5 pA threshold. Right panel compares one of the simulated control distributions (black line) to real data recorded from V1m in the control hemisphere (pink line). **B.** To simulate perfect scaling we multiplied one of the control distributions (shown in green in A) by 1.20 (scaling factor). We applied this scaling factor to the un-truncated distributions (left panel, black line indicates un-scaled control distribution, red line indicates distribution scaled by 1.20). To compare to real data, both the control and scaled distributions were then truncated at the 5 pA detection threshold (vertical dashed line, right panel). **C.** We applied our standard analysis method to detect synaptic scaling to these simulated distributions. The result obtained is similar to real data and the scaling factor estimate from the linear fit procedure (left panel, red solid line) is close to the real scaling factor (1.22 vs 1.20). The intercept for this simulated multiplicative scaling is close to 0, similar to our real data (-0.852 for simulation vs +0.318 for real data, see Figure S3H). Gray dashed line is the unity line. The right panel shows that the scaled distribution (red solid line) can then be down-scaled by the estimated scaling factor (red dashed line). This, when combined with application of the detection threshold to the down-scaled distribution, accurately recovers the control distribution (black line).

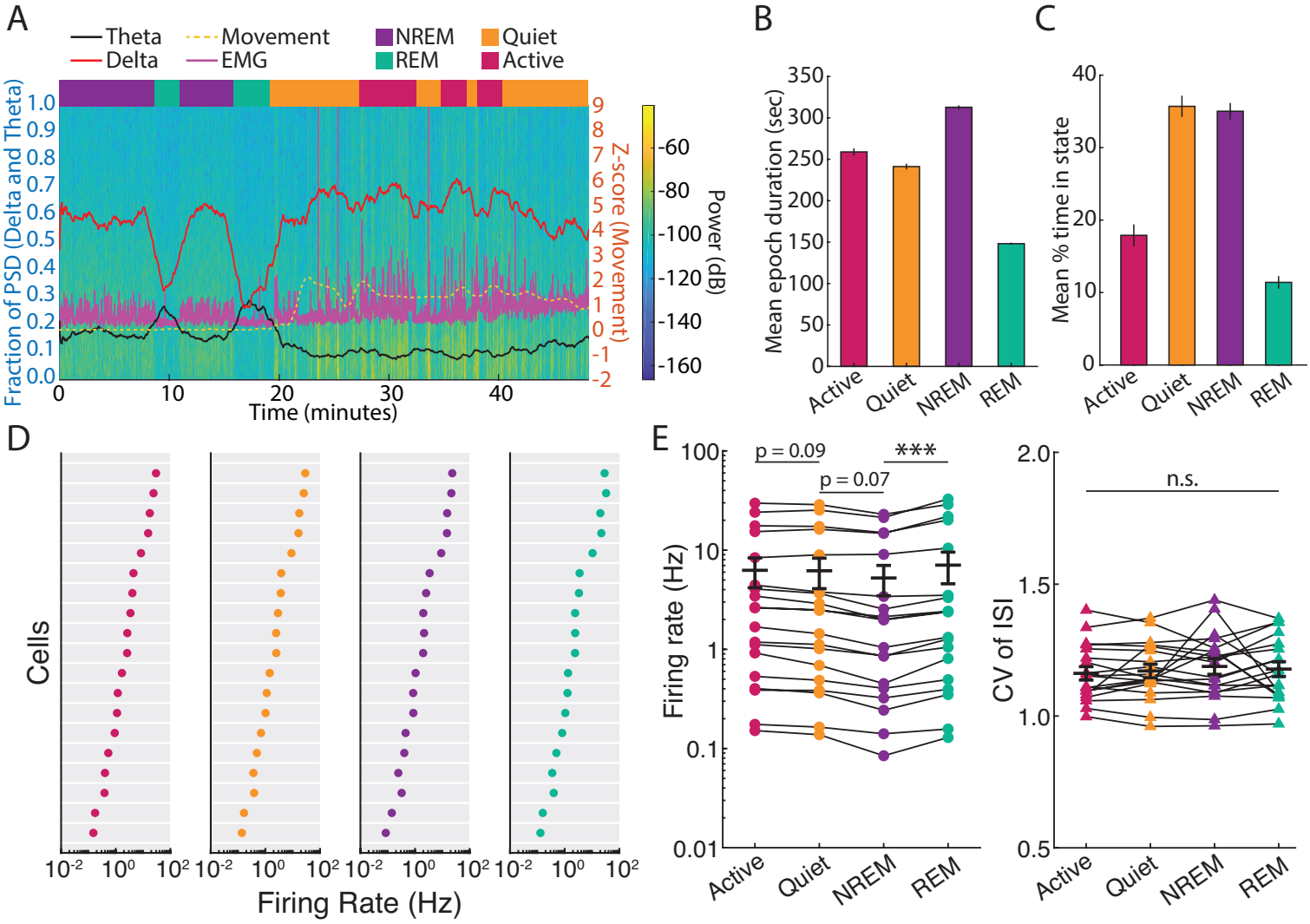
A
Theta
Delta
Movement
EMG
NREM
REM
Quiet
Active
Fraction of PSD (Delta and Theta)
Z-score (Movement)
Power (dB)
Time (minutes)
B
Mean epoch duration (sec)
Active
Quiet
NREM
REM
C
Mean % time in state
D
Cells
Firing Rate (Hz)
E
p = 0.09
p = 0.07
***
Firing rate (Hz)
n.s.
CV of ISI

Figure S5: Behavioral state scoring and FR differences across states, Related to Figures 4 and 5. **A.** Example behavioral scoring for a ~30-minute period. Background spectrogram is the LFP power between 0.3 and 15 Hz (colorbar on the right). Red and black line represent the fraction of power in the delta (0.3 – 4 Hz) and theta (5 – 8 Hz) bands (plotted on left y-axis). Blue and violet dashed lines are EMG and movement values, z-scored to the 60-minute block being scored (plotted on right y-axis). Colored rectangles at the top show the scored state after manual correction of random forest classifier output (NREM sleep, REM sleep, Active wake or Quiet wake). **B.** Mean epoch duration for each behavioral state for all animals. **C.** Average percent time in each state for all animals. **D.** Mean FR of every RSU recorded in the control hemisphere in each state, ranked by mean FR in active wake. **E.** Left, Average FR in each state for RSUs recorded in the control hemisphere, normalized for each neuron to the mean FR in active wake. Right, mean coefficient of variation (CV) of the inter-spike interval (ISI) in each state. Gray horizontal lines connect the same neurons' FR across states. ***, p = 0.001; paired Wilcoxon sign-rank tests with Bonferroni correction.

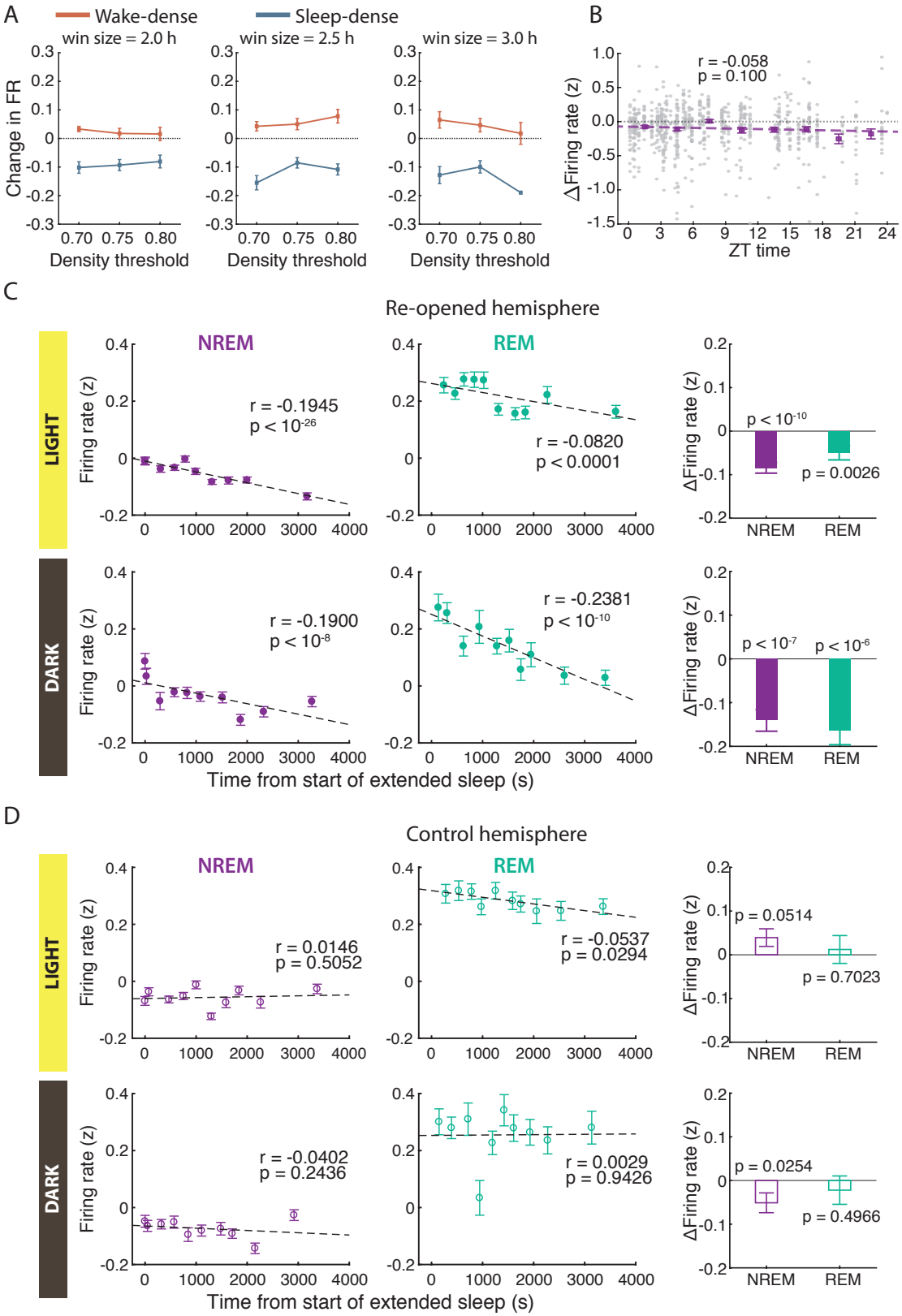
A
Wake-dense
Sleep-dense
win size = 2.0 h
win size = 2.5 h
win size = 3.0 h
Change in FR
Density threshold
B
r = -0.058
p = 0.100
ΔFiring rate (z)
ZT time
C
Re-opened hemisphere
LIGHT
DARK
NREM
REM
Firing rate (z)
r = -0.1945
p < 10-26
r = -0.0820
p < 0.0001
r = -0.1900
p < 10-8
r = -0.2381
p < 10-10
ΔFiring rate (z)
p < 10-10
p = 0.0026
p < 10-7
p < 10-6
Time from start of extended sleep (s)
D
Control hemisphere
r = 0.0146
p = 0.5052
r = -0.0537
p = 0.0294
r = -0.0402
p = 0.2436
r = 0.0029
p = 0.9426
p = 0.0514
p = 0.7023
p = 0.0254
p = 0.4966

Figure S6: Result of sleep-related analyses do not depend on chosen parameters or circadian time, Related to Figure 5. **A.** Mean change in FR for RSUs in the re-opened hemisphere in sleep- and wake-dense windows for different density thresholds to estimate FR change (see STAR Methods, “FR analyses”). The analysis was repeated for 2-hour (left), 2.5-hour (center) and 3-hour (right) windows. Density threshold is minimum % time in sleep- or wake- for a window to be considered sleep- or wake-dense. **B.** Correlation between change in FR over extended sleep periods and circadian time (expressed in Zeitgeber Time, hour 0 = lights ON, hour 12 = lights OFF). Gray circles represent change in FR over individual extended sleep periods. Purple squares show mean change in FR ± SEM across all epochs, averaged in 3-hour bins. Gray dotted lines indicates no change. Pearson correlation was calculated on the non-binned dataset. All values calculated during the 48-hour period of homeostatic recovery. **C.** Extended sleep analysis (same as Figure 5) for re-opened hemisphere neurons, split by Light (top row) and Dark (bottom row). Plots show z-scored FR in NREM (purple) and REM (green) episodes during extended sleep as a function of when those episodes occurred since the start of extended sleep. Data were grouped into 10 equally-sized groups for visualization purposes. Pearson correlations and p-values were computed on the non-grouped data. Bar plots on the right show the difference in FR between the last and first NREM (purple) and REM (green) episodes in each extended sleep period. Significance for the bar plots was assessed using one-sample t-tests vs a mean of 0. **D.** As in C, for control hemisphere data.

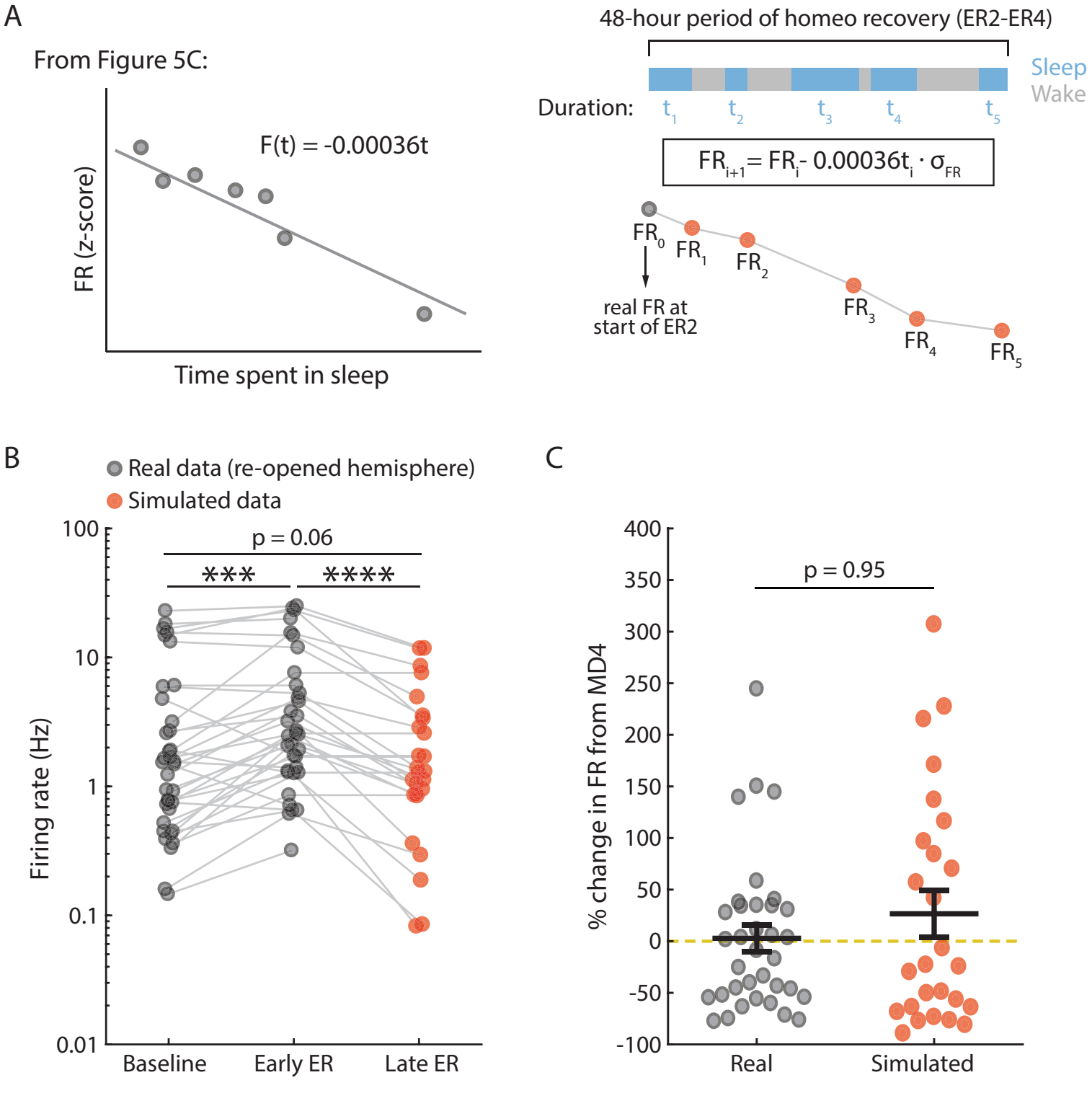
A
From Figure 5C:
F(t) = -0.00036t
FR (z-score)
Time spent in sleep
48-hour period of homeo recovery (ER2-ER4)
Sleep
Wake
Duration:
t1
t2
t3
t4
t5
FRi+1 = FRi - 0.00036ti · σFR
FR0
FR1
FR2
FR3
FR4
FR5
real FR at start of ER2
B
Real data (re-opened hemisphere)
Simulated data
p = 0.06
***
****
Firing rate (Hz)
100
10
1
0.1
0.01
Baseline
Early ER
Late ER
C
p = 0.95
% change in FR from MD4
400
350
300
250
200
150
100
50
0
-50
-100
Real
Simulated

Figure S7. FR changes observed during sleep are sufficient to account for homeostatic recovery, Related to Figure 5. **A.** Diagram of simulation. From the correlation between FR in NREM and time from the start of extended sleep (Figure 5C), we found the relationship between z-scored FR and time in sleep. Firing rate as a function of time can be expressed as $F(t) = -0.00036t$. For each animal, we found the sequence of sleep-wake states during the 48-hour period during which homeostatic recovery is observed (experiment days ER2-ER3). We then assumed that FRs were not changing during wake, and calculated the change in FR across sleep epochs based on the equation above and the duration of each sleep epoch (t1, t2, etc.). Since the equation above expresses a change in z-scored FR, we calculated the experiment-wide standard deviation of the FR for each neuron in our dataset. We then computed each neurons' real FR in the 2-hours prior to the beginning of the homeostatic period (FR_0). Using these two values, we computed the FR of each neuron after each sleep period (FR_1, FR_2, etc.). The final value thus obtained was used as the simulated FR on ER4 (Late ER). Neurons whose FR did not increase by at least 1 SD after ER were not scaled down in the simulation. **B.** Plot showing real FRs for each neuron in our dataset at Baseline and Early ER (gray circles), followed by the simulated value for the FR of each neuron in Late ER based on the calculation described in A (red circles). While the change in activity over each sleep episode is small, the cumulative change is enough to account for the observed homeostatic recovery, and in fact we obtain a slight over-estimate of such recovery, though the simulated Late ER data is not significantly different from the real Baseline data ($p = 0.06$, Sign-rank test). Light gray lines connect each neurons' FR across time. Missing circles in Late ER result from FRs dropping below 0 in the calculation above. **C.** Percent change in FR between MD4 and ER4 (Baseline vs Late ER) for real and simulated data. $p = 0.95$, two-sample t-test.

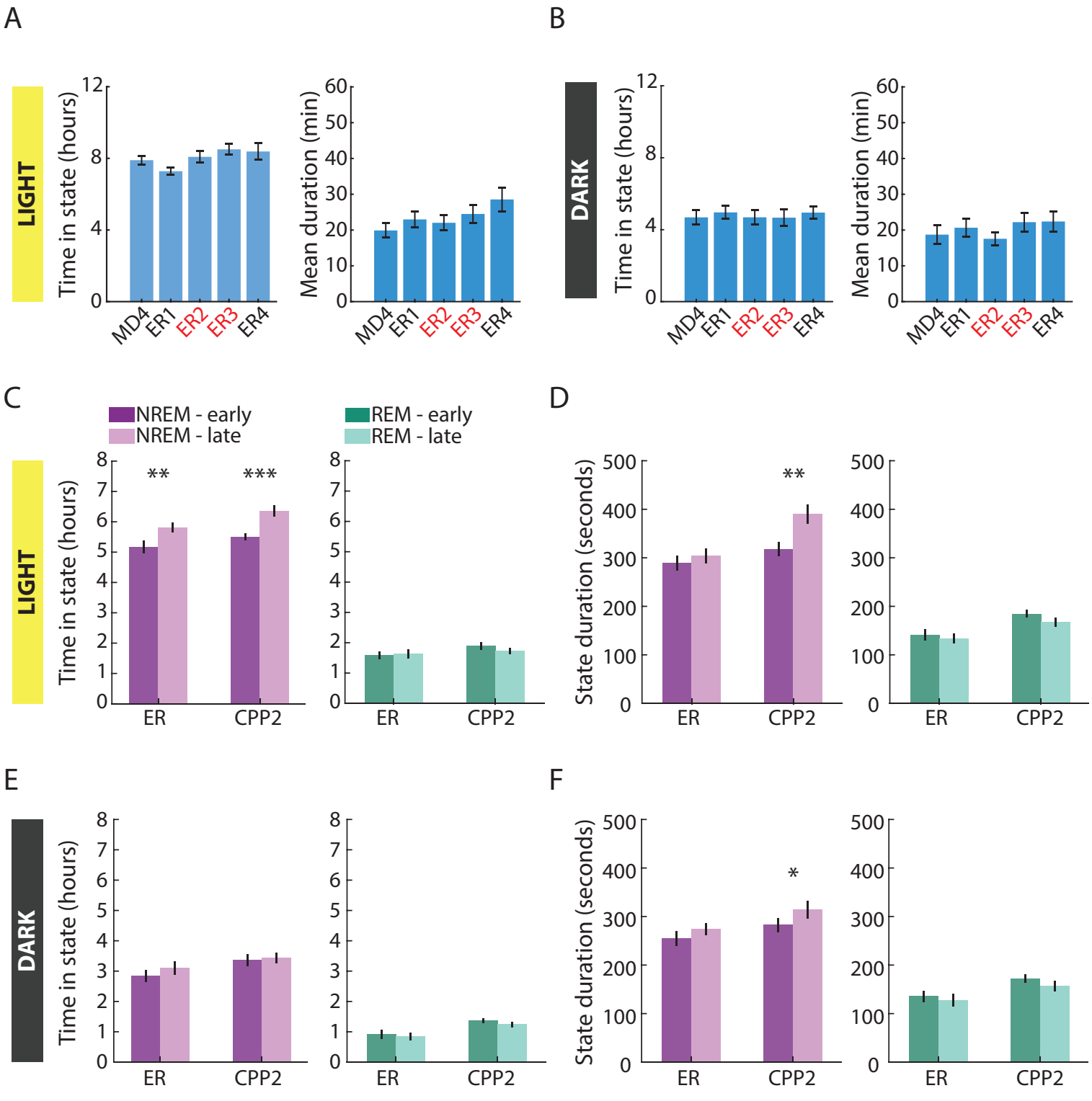
A
B
LIGHT
DARK
Time in state (hours)
Mean duration (min)
MD4
ER1
ER2
ER3
ER4
C
D
E
F
NREM - early
NREM - late
REM - early
REM - late
State duration (seconds)
ER
CPP2
**
***
*

Figure S8. CPP injections do not drastically alter sleep architecture, Related to Figure 2. **A.** Left, Average time spent in sleep for CPP injected animals, during the 12-hour light phase in each day of the experiment from MD4 to ER4. Right, Mean duration of sleep episodes on each day. CPP injections occurred at the beginning of the light phase on ER2 and ER3 (red labels on the x-axis). No significant differences, One-way ANOVA with Tukey-Kramer post-hoc. **B.** As in A, but for the 12-hour dark phase of each day. **C.** Mean time spent in NREM (purple) or REM (green) early (days MD4-ER1, dark colors) or late (days ER2-ER3, light colors) in the experiment, during the 12-hour light phase, regular eye re-opening experiments (ER) and eye re-opening with CPP injections on ER2 and ER3 (CPP2). **, $p < 0.01$; ***, $p < 0.001$; two-sample t-test. **D.** Mean duration of NREM (purple) or REM (green) states early (days MD4-ER1, dark colors) or late (days ER2-ER3, light colors) in the experiment, during the 12-hour light phase, for ER and CPP2 datasets. **, $p < 0.01$; two-sample t-test. **E.** As in C, for 12-hour dark phases. **F.** As in D, for 12-hour dark phases. *, $p < 0.05$; two-sample t-test.